Available online at www.sciencedirect.com
SCIENCE DIRECT®
Neuroscience Letters 364 (2004) 11–15
Neuroscience Letters
www.elsevier.com/locate/neulet

# Axonal regrowth downregulates the synthesis of glial cell line-derived neurotrophic factor in the lesioned rat sciatic nerve

Yoshihisa Yamada[a,b], Katsuji Shimizu[b], Atsumi Nitta[a], Hitomi Soumiya[a], Hidefumi Fukumitsu[a], Shoei Furukawa[a,*]

[a] *Laboratory of Molecular Biology, Gifu Pharmaceutical University, Mitahora-higashi 5-6-1, Gifu 502-8585, Japan*
[b] *Department of Orthopaedic Surgery, Gifu University, Tsukasa-machi 40, Gifu 500-8705, Japan*

Available online at www.sciencedirect.com
SCIENCE DIRECT®
Neuroscience Letters 364 (2004) 11–15
Neuroscience Letters
www.elsevier.com/locate/neulet

# Axonal regrowth downregulates the synthesis of glial cell line-derived neurotrophic factor in the lesioned rat sciatic nerve

Yoshihisa Yamada[a,b], Katsuji Shimizu[b], Atsumi Nitta[a], Hitomi Soumiya[a], Hidefumi Fukumitsu[a], Shoei Furukawa[a,*]

[a] *Laboratory of Molecular Biology, Gifu Pharmaceutical University, Mitahora-higashi 5-6-1, Gifu 502-8585, Japan*
[b] *Department of Orthopaedic Surgery, Gifu University, Tsukasa-machi 40, Gifu 500-8705, Japan*

Received 18 December 2003; received in revised form 16 March 2004; accepted 22 March 2004

**Abstract**

The effect of axonal regeneration on de novo synthesis of glial cell line-derived neurotrophic factor (GDNF) in rat sciatic nerves was examined. Transection of the sciatic nerve caused a prominent increase in the GDNF content in the distal segments within 1 week. The high level was sustained until 4 weeks in the animal model in which the nerve ends were ligated with thread (non-regeneration group); however, it was reduced to the original level within 2 or 4 weeks after the transection only in the segments invaded by regenerating axons in the models in which the nerve ends were coaptated (regeneration group). Expression of both GDNF protein and mRNA was decreased with a reciprocal increase in the density of neurofilaments, used as a marker of axonal ingrowth in distal segments of the regeneration group, suggesting that axonal contact turned off the GDNF-mediated nerve regeneration activity.


*Keywords:* Glial cell line-derived neurotrophic factor (GDNF); Synthesis; Injury; Nerve regeneration; Sciatic nerve; Enzyme immunoassay (EIA)

Peripheral nerve regeneration comprises the formation of axonal sprouts, their outgrowth as regenerating axons, and the reinnervation of original targets; and these processes depend, predominantly on the biological actions of diffusible neurotrophic factors. Injury of peripheral nerves induces de novo synthesis of neurotrophic factors, including nerve growth factor (NGF), brain-derived neurotrophic factor (BDNF), and glial cell line-derived neurotrophic factor (GDNF), in the distal part of the injury [2,10,14,15]; and the factors thus accumulated play roles in axonal sprouting from the proximal stump, growth of these sprouts into the distal nerve segment, and their extension to the targets. A Schwann cell column is formed after removal of damaged myelin sheaths by macrophages, and it becomes an indispensable pathway for regenerating axons to grow through to the target [6]. Schwann cells and their basal lamina serve as the source of neurotrophic factors and/or the scaffold for regenerating axons through interactions with a variety of receptors and adhesion molecules [6,18]. However, the critical mechanisms by which peripheral nerve regeneration is achieved are not fully understood.

GFRα1 molecules, which are glycosyl-phosphatidylinositol-anchored receptors for GDNF, have recently pointed to additional functions of nerve regeneration. Although both GFRα1 and c-Ret, a tyrosine kinase that binds to the GFRα1–GDNF complex and transduces signals of the GDNF family, are required for responsiveness to GDNF family ligands, GFRα1 functions to capture GDNF and present it in *trans* fashion to c-Ret receptors [10]. GFRα1 elicits both long-range and localized guidance effects by creating positional information for c-Ret-expressing axons in the presence of GDNF [10]. Soluble GFRα1 can be released from cultured neurons, Schwann cells and explants of the sciatic nerve [17], and GDNF and GFRα1 mRNA expression is facilitated in the Schwann cells of the distal part of the injured sciatic nerve [5,10,15]. The coexistence of both GFRα1 and GDNF in the injured sciatic nerve strongly suggests that GFRα1–GDNF complexes predominantly facilitate nerve regeneration of c-Ret-expressing dorsal root ganglion neurons and spinal motoneurons by acting through an axonal guidance mechanism. The regulatory role of GFRα1 has been postulated from the results

* Corresponding author. Tel.: +81-58-237-3931; fax: +81-58-237-8589.
*E-mail address:* furukawa@gifu-pu.ac.jp (S. Furukawa).

0304-3940/$ – see front matter © 2004 Elsevier Ireland Ltd. All rights reserved.
doi:10.1016/j.neulet.2004.03.078

of detailed in vitro experiments [10], but the role of GDNF synthesis has not yet been fully evaluated.

In this study, we monitored the expression of GDNF protein and mRNA during degeneration and regeneration of the rat sciatic nerve, and found them to decrease coincidentally with the ingrowth of the regenerating axons.

All experiments with animals were carried out according to the guidelines of animal experimentation of the NIH Guide for Care and Use of Laboratory Animals. Male Wistar rats (7 weeks old, 150–180 g, Nippon SLC, Shizuoka, Japan) were divided into two groups and anesthetized with sodium pentobarbital (60 mg/kg, i.p.). In one group (non-regeneration group), the right sciatic nerve was cut distal to the obturator tendon, and both ends were ligated with 4-0 silk threads to prevent nerve regeneration. In the other group (regeneration group), the right sciatic nerve was cut at the same point, and both ends were immediately coaptated with 10-0 nylon threads under a dissecting microscope. At the appropriate time the animals were sacrificed under deep anesthesia with diethyl ether, and their sciatic nerves were dissected out and cut into six segments, each of 10-mm length. These procedures were schematically illustrated in Fig. 1.

Human recombinant GDNF was donated by Amgen (Thousand Oaks, CA, USA). GDNF (0.5 mg) dissolved in saline was emulsified with Freund's complete adjuvant and injected intradermally into rabbits four times at 2-week intervals. Blood was collected 1 week after the final injection. Specific antibodies were purified similarly as reported for anti-NGF antibodies [8], and used for coating of wells or preparation of biotinylated antibodies for enzyme immunoassay (EIA). The detection limit of our EIA system was as low as 4.0 pg/ml, dose-dependent below 1000 pg/ml, and specific for GDNF among other GDNF family proteins,

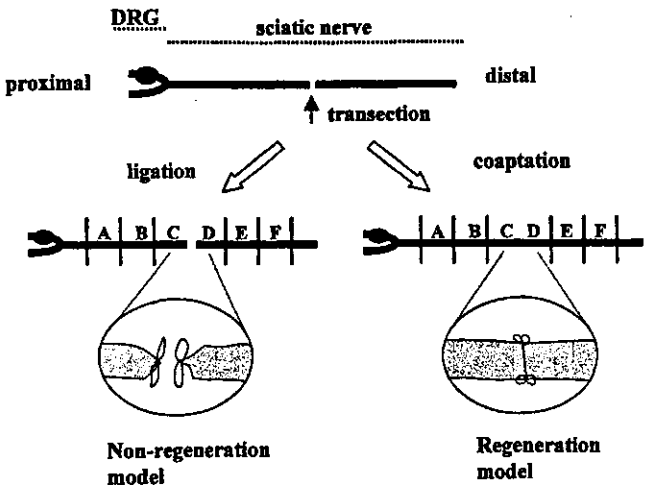


Fig. 1. A schematic representation of the location of the segments used for experiments. The sciatic nerves were dissected out and cut into six segments, each of 10-mm length. Each segment was alphabetically ordered from central to peripheral side. Transection site between segments C and D is indicated by the arrow. DRG: dorsal root ganglion.

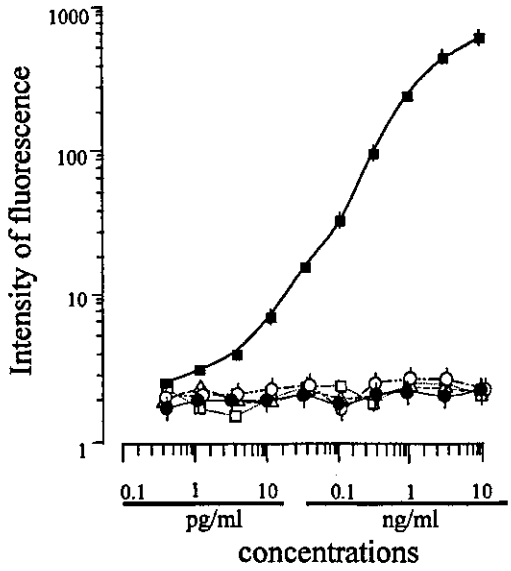


Fig. 2. Calibration curves generated for GDNF family proteins and TGF-β1 by use of the EIA system. Various concentrations of GDNF (■), neurturin (□), persephin (△), arteminm (○), and TGF-β1 (●) were applied to the EIA system for GDNF developed similarly as EIA systems for neurotrophins [16]. In short, 96-multiwell plates (Beckton Dickinson) were coated with anti-GDNF antibodies and blocked with 1% skim milk. Test samples were incubated in the antibody-coated wells. Biotinylated anti-GDNF specific antibodies were reacted with antigens bound to the wells, and these antibodies were then reacted with avidin-conjugated β-D-galactosidase (Boehringer Mannheim, Germany). Finally, the bound enzyme activity was measured by using a fluorogenic substrate, 4-methylumbelliferyl-β-D-galactoside. The standard curve of GDNF was used to determine the concentration. Each value is expressed as the mean ± S.E. of triplicate determinations. The S.E. is not shown when it is less than the width of the symbol.

including artemin, neurturin, persephin, and transforming growth factor (TGF)-β, the latter being the prototype of the super family (Fig. 2). The GDNF mRNA level was estimated by the reverse transcription-polymerase chain reaction (RT-PCR) as described earlier [7].

It was earlier shown that transection of the sciatic nerve induced a drastic increase in GDNF expression in Schwann cells located distal to the injury [5,12,15]. Neurofilaments are present in regenerating myelinated axons and larger unmyelinated axons [4], therefore, they were used as an indicator of the regenerating axons. Multiple bands of neurofilaments with about 160 kDa were found in the proximal all segments in the regeneration and non-regeneration models at all times tested. The bands appeared in the distal segments D, E, or F with the increase of the times after transection in the regeneration models, but did not in those of the non-regeneration models, demonstrating that the ingrowth of the regenerating axons occurred in the sciatic nerve of the regenerating group (Fig. 3-II). There was no difference in GDNF content between the regenerating and non-regenerating sciatic nerve up to 1 week after the surgery (Fig. 3-I). Neurofilaments were not detected in the distal stumps of either group at that time, demonstrating

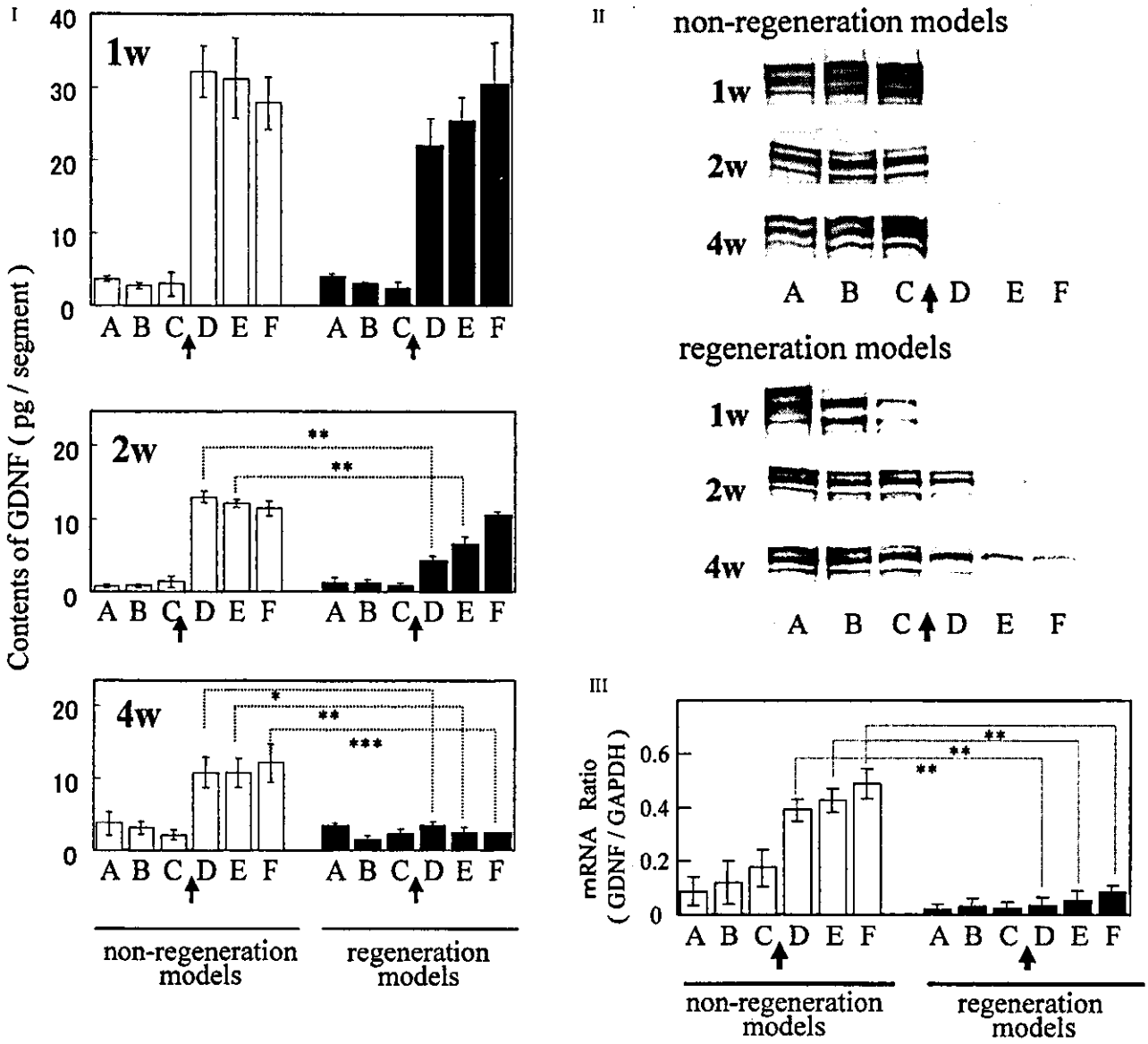


Fig. 3. Effects of nerve regeneration on the injury-induced increase in GDNF and its mRNA in the sciatic nerve segments. (I) Distribution of GDNF protein in the sciatic nerves of the regeneration (right) and non-regeneration (left) models. Each segment was pulse-sonicated in 0.1 M Tris–HCl buffer, pH 7.4, containing 1 M NaCl, 2 % bovine serum albumin, 2 mM EDTA, 80 units aprotinin/l, and 0.02% $NaN_3$. The supernatant fluids after centrifugation were subjected to the EIA to measure GDNF and to Western immunoblotting for neurofilaments. GDNF content is expressed as bars with the means ± S.E. of six to nine animals. Open bars indicate the values of the non-regeneration group; and closed bars, those of the regeneration group. Significance: $^{*}P < 0.05$, $^{**}P < 0.01$, $^{***}P < 0.001$ vs. the value of corresponding segment of non-regeneration group (ANOVA with Tukey post hoc). (II) Distribution of neurofilaments in the sciatic nerve segments of non-regeneration (upper) and regeneration (lower) models. The supernatant fluids of tissue homogenates were electrophoresed in an SDS polyacrylamide gel, and the proteins were then transferred to PVDF membranes (Fluorotrans™, Nihon Genetics). Neurofilaments were visualized by using anti-neurofilament 160 mouse antibody (Sigma, St. Louis, MO, USA) as described earlier [1]. The photographs shown are representatives of those of three independent experiments. (III) GDNF mRNA expression of the non-regeneration (left) and regeneration (right) models. Total RNA was transcribed into cDNAs as described previously [7]. cDNAs of GDNF and glyceraldehyde 3-phosphate dehydrogenase (GAPDH) were optimally amplified with an Advantage 2 PCR Kit (Clontech) using primers specific for GDNF [12] and GAPDH [20]. The values are the means ± S.E. of the ratio of the intensity of GDNF product to that of GAPDH product obtained from an identical RNA sample ($n = 4$). Open bars indicate the values of the non-regeneration group; and the closed bars, those of the regeneration group. Significance: $^{**}P < 0.001$ vs. the value corresponding to the segment of the non-regeneration group (ANOVA with Tukey post hoc).

no ingrowth of regenerating nerves (Fig. 3-II). The GDNF level was significantly reduced 2 weeks after the surgery in the distal segments D and E of the regeneration group, in which neurofilaments were detected. However, GDNF level was unchanged in the most distal segment, segment F, yet lacking in neurofilaments. Four weeks after the operation, the reduction in the GDNF level expanded to segment F in the regeneration group; but the GDNF level still remained high in the non-regeneration group (Fig. 3-I). The reduction in the GDNF level was limited to the distal segments

containing neurofilaments (Fig. 3-II). Furthermore, the GDNF mRNA expression was reduced in all segments D, E, and F of the regeneration group when compared with that in the same segments of the non-regeneration group (Fig. 3-III). These observations suggest that the injury-induced increase in GDNF synthesis in the distal stump is negatively regulated by interactions between regenerating axons and GDNF-producing cells, i.e., Schwann cells. A gradient of GDNF formed in the distal stump may drive more rapidly and guide more effectively the growth cones of regenerating axons to the target end tissues.

In the present study, we demonstrated that the lesion-induced enhancement of GDNF synthesis was restored to the original level coincidentally with axonal ingrowth into the distal stumps. This finding suggests that axonal contact attenuates GDNF synthesis and that the lesion-enhanced GDNF synthesis is aimed at accelerating nerve regeneration, which would explain why the GDNF synthesis is low in the proximal part of the injured nerve and in the intact peripheral nerve.

Interestingly, a recent study demonstrated that exogenous GFRα1 protein potentiated neurite outgrowth of cultured embryonic sensory or sympathetic neurons and acted as a long-range directional cue by creating positional information for c-Ret-expressing axons only in the presence of GDNF [10]. As the neurites within the sciatic nerve predominantly run from sensory neurons of the dorsal root ganglia and motoneurons of the spinal cord, most of regenerating neurites express c-Ret. Moreover, GDNF was shown to act as a peripheral signal, thereby regulating both the position of motoneurons and their muscle innervation [3]. Therefore, GDNF or GFRα1–GDNF complexes produced by Schwann cells distal to the lesion site of peripheral nerves are likely to play important roles in axonal regeneration and guidance of c-Ret-expressing neurons. Our present results, that axonal ingrowth suppressed GDNF expression, lead us to propose that the GDNF-mediated regeneration/guidance system elaborated by Schwann cells is disengaged by axonal contact with Schwann cells. This may be the first in vivo evidence that regenerating axons halt the machinery driving nerve regeneration.

The mechanisms underlying the contact behavior of Schwann cell–axon association are not yet fully understood. A recent study indicated that excitation by axons increased the number of acetylcholine receptors on Schwann cells [13]. Others showed that TGF-β, a molecule known to be released from axon terminals, upregulated expression of laminin/collagen receptor, α1β1 integrin [19], or leukemia inhibitory factor on cultured Schwann cells [11]. The involvement of TGF-β in the regulatory mechanism of GDNF gene expression may be plausible, because gene expression of α1β1 integrin or leukemia inhibitory factor is upregulated in the distal nerve stump of the injured sciatic nerves as well as GDNF expression [11,19]. Moreover, Kinameri and Matsuoka [9] reported that treatment of the Schwann cells isolated from the sciatic nerve with combination of bone morphogenetic protein-2 (BMP2) and retinoic acid (RA) dramatically induced GDNF-mRNA, while BMP2 or RA alone had no effect. They also found that in the explant culture as an in vitro lesion model, sciatic nerve segments began to express mRNA for BMP2 concomitantly with the induction of GDNF mRNA. These suggest that the Schwann cell-produced BMP2 induces GDNF after nerve injury in an autocrine fashion. Therefore, ingrowing axons may down-regulate BMP2 and/or TGF-β. However, a direct interaction between Schwann cells and ingrowth axons could not be completely excluded from a possible mechanism.

Further studies are needed to identify the molecular entities that regulate GDNF synthesis in Schwann cells in vivo; and to clarify the physiological roles of GDNF in degeneration and regeneration processes in the peripheral nervous system.

## References

[1] H. Fukumitsu, Y. Furukawa, M. Tsusaka, H. Kinukawa, A. Nitta, H. Nomoto, T. Mima, S. Furukawa, Simultaneous expression of brain-derived neurotrophic factor and neurotrophin-3 in Cajal-Retzius, subplate and ventricular progenitor cells during early development stages of the rat cerebral cortex, Neuroscience 84 (1998) 115–127.
[2] H. Funakoshi, J. Frisen, G. Barbany, T. Timmusk, O. Zachrisson, V.M. Verge, H. Persson, Differential expression of mRNAs for neurotrophins and their receptors after axotomy of the sciatic nerve, J. Cell Biol. 123 (1993) 55–65.
[3] G. Haase, E. Dessaud, A. Garces, B. de Bovis, M. Birling, P. Filippi, H. Schmalbruch, S. Arber, O. deLapeyriere, GDNF acts through PEA3 to regulate cell body positioning and muscle innervation of specific motor neuron pools, Neuron 35 (2002) 893–905.
[4] S.M. Hall, A.P. Kent, R. Curtis, D. Robertson, Electron microscopic immunocytochemistry of GAP-43 within proximal and chronically denervated distal stumps of transected peripheral nerve, J. Neurocytol. 21 (1992) 820–831.
[5] A. Hoke, C. Cheng, D.W. Zochodne, Expression of glial cell line-derived neurotrophic factor family of growth factors in peripheral nerve injury in rats, Neuroreport 11 (2000) 1651–1654.
[6] C. Ide, Peripheral nerve regeneration, Neurosci. Res. 25 (1996) 101–121.
[7] H. Ito, A. Nakajima, H. Nomoto, S. Furukawa, Neurotrophins facilitate neuronal differentiation of cultured neural stem cells via induction of mRNA expression of basic helix-loop-helix transcription factors Mash1 and Math1, J. Neurosci. Res. 71 (2002) 648–658.
[8] K. Kaechi, Y. Furukawa, R. Ikegami, N. Nakamura, F. Omae, Y. Hashimoto, K. Hayashi, S. Furukawa, Pharmacological induction of physiologically active nerve growth factor in rat peripheral nervous system, J. Pharmacol. Exp. Ther. 264 (1993) 321–326.
[9] E. Kinameri, I. Matsuoka, Autocrine action of BMP2 regulates expression of GDNF-mRNA in sciatic Schwann cells, Mol. Brain Res. 117 (2003) 221–227.
[10] F. Ledda, G. Paratcha, C.F. Ibanez, Target-derived GFRalpha1 as an attractive guidance signal for developing sensory and sympathetic axons via activation of Cdk5, Neuron 36 (2002) 387–401.
[11] I. Matsuoka, A. Nakane, K. Kurihara, Induction of LIF-mRNA by TGF-beta 1 in Schwann cells, Brain Res. 776 (1997) 170–180.
[12] N. Matsushita, Y. Fujita, M. Tanaka, T. Nagatsu, K. Kiuchi, Cloning and structural organization of the gene encoding the mouse glial cell line-derived neurotrophic factor, GDNF, Gene 203 (1997) 149–157.
[13] G.V. Maximov, V.V. Revin, I.P. Grunyushkin, O.R. Kols, Role of acetylcholine in regulation of interaction between axon and

Schwann cell during rhythmic excitation of nerve fibers, Biochemistry (Moscow) 65 (2000) 431–435.
[14] M. Meyer, I. Matsuoka, C. Wetmore, L. Olson, H. Thoenen, Enhanced synthesis of brain-derived neurotrophic factor in the lesioned peripheral nerve: different mechanisms are responsible for the regulation of BDNF and NGF mRNA, J. Cell Biol. 119 (1992) 45–54.
[15] P. Naveilhan, W.M. ElShamy, P. Ernfors, Differential regulation of mRNAs for GDNF and its receptors Ret and GDNFR alpha after sciatic nerve lesion in the mouse, Eur. J. Neurosci. 9 (1997) 1450–1460.
[16] A. Nitta, M. Ohmiya, T. Jin-nouchi, A. Sometani, T. Asami, H. Kinukawa, H. Fukumitsu, H. Nomoto, S. Furukawa, Endogenous neurotrophin-3 is retrogradely transported in the rat sciatic nerve, Neuroscience 8 (1999) 679–685.
[17] G. Paratcha, F. Ledda, L. Baars, M. Coulpier, V. Besset, J. Anders, R. Scott, C.F. Ibanez, Released GFRalpha1 potentiates downstream signaling, neuronal survival, and differentiation via a novel mechanism of recruitment of c-Ret to lipid rafts, Neuron 29 (2001) 171–184.
[18] Y. Shibuya, A. Mizoguchi, M. Takeichi, K. Shimada, C. Ide, Localization of N-cadherin in the normal and regenerating nerve fibers of the chicken peripheral nervous system, Neuroscience 67 (1995) 253–261.
[19] H.J. Stewart, D. Turner, K.R. Jessen, R. Mirsky, Expression and regulation of alpha1beta1 integrin in Schwann cells, J. Neurobiol. 33 (1997) 914–928.
[20] H. Wong, W.D. Anderson, T. Cheng, K.T. Riabowol, Monitoring mRNA expression by polymerase chain reaction: the "primer-dropping" method, Anal. Biochem. 223 (1994) 251–258.

# Developmental Shift in Bidirectional Functions of Taurine-Sensitive Chloride Channels during Cortical Circuit Formation in Postnatal Mouse Brain

**Mika Yoshida, Satoshi Fukuda, Yusuke Tozuka, Yusei Miyamoto, Tatsuhiro Hisatsune**

Department of Integrated Biosciences, University of Tokyo, Bioscience Bldg. 402, Kashiwa, Chiba 277-8562, Japan

*Received 29 September 2003; accepted 3 November 2003*

**ABSTRACT:** **Taurine (2-aminoethanesulfonic acid) is the most abundant free amino acid in the developing mammalian cerebral cortex, however, few studies have reported its neurobiological functions during development. In this study, by means of whole-cell patch-clamp recordings, we examined the effects of taurine on chloride channel receptors in neocortical neurons from early to late postnatal stages, which cover a critical period in cortical circuit formation. We show here that taurine activates chloride channels in cortical neurons throughout the postnatal stages examined (from postnatal day 2 to day 36). The physiological effects of taurine changed from excitatory to inhibitory due to variations in the intracellular $Cl^-$ concentration during development. An antagonist blocking analysis also demonstrated a developmental shift in the receptor target of taurine, from glycine receptors to $GABA_A$ receptors. Taken together, these results may reflect genetically programmed, bidirectional functions of taurine. At the early developmental stage, taurine acting on glycine receptors would serve to promote cortical circuit formation. As cortical circuit has to be regulated in the later stages, taurine would serve as a safeguard against hyperexcitable circuit.** © 2004 Wiley Periodicals, Inc. J Neurobiol 60: 166–175, 2004

*Keywords:* **circuit formation; depolarization; gramicidin perforated-patch recording; neuro-protective function; whole-cell patch recording**

## INTRODUCTION

Taurine (2-aminoethanesulfonic acid) is one of the most abundant free amino acids in the developing nervous system (Huxtable, 1989). In mammals, sufficient taurine for embryonic development is received from the mother via the placenta, while neonates obtain taurine from mothers' milk (Sturman et al., 1977; Sturman, 1981; Chesney, 1985). Taurine is structurally similar to the inhibitory transmitter gamma-aminobutyric acid (GABA) and glycine. It has been shown that taurine interacts both GABA- (Malminen and Kontro, 1986, 1987) and glycine-receptors (Kontro and Oja, 1987a, b), and induces chloride-currents in neurons (Linne et al., 1996; Ye et al., 1997; Flint et al., 1998; Puopolo et al., 1998; del Olmo et al., 2000; Mori et al., 2002).

At the developing neocortex of the early developmental stage, nonsynaptically released taurine activates glycine-receptors (Flint et al., 1998). In a previous study, we have demonstrated that the taurine-dependent activation of glycine-receptors contributes to $Ca^{2+}$ influx via synaptic activation of NMDARs (N-methyl-D-aspartate receptors) (Miyakawa et al., 2002). Crair and Malenka (1995) elegantly demonstrated that synaptic activation of NMDARs is criti-

*Correspondence to:* T. Hisatsune (hisatsune@k.u-tokyo.ac.jp).

Contract grant sponsor: Grant-in Aid for Scientific Research from the Ministry of Education, Science, Sports and Culture of Japan.

Contract grant sponsor: The Food Science Institute Foundation (T.H.).



Published online 16 April 2004 in Wiley InterScience (www.interscience.wiley.com).
DOI 10.1002/neu.20003

cally important for the developmental plasticity of cortical circuitry. Although, in a mature cortical neuron, the voltage-dependent block of NMDARs was released by the activation of alpha-amino-3-hydroxy-5-methyl-4-isoxazolepropimate (AMPA)-type glutamate-receptors, in an immature neuron of the developing neocortex, the expression levels of AMPA receptors would not be enough to activate NMDARs (Liao et al., 1995; Isaac et al., 1997). Ben-Ari et al. first demonstrated that the depolarizing action of chloride channels compensates for the lack of AMPA receptors in an immature neuron of developing hippocampus (Ben-Ari et al., 1989, 1997). At the developing neocortex, the neurochemical machinery for the activation of NMDAR still remained unclear. The major aim of this study is to ascertain our hypothesis that taurine, which is present at extremely high levels in the developing neocortex, activates chloride receptors then depolarizes the responding immature neuron.

In the present study, the properties of taurine-sensitive receptor channels in neocortical neurons from early to late postnatal stages have been examined by means of whole-cell patch-clamp recordings. To evaluate whether the opening of taurine-sensitive receptor channels would lead to depolarization or hyperpolarization of the responding neuron, gramicidin-perforated patch-clamp recordings (Owens et al., 1996) were also carried out. The physiological effects of taurine changed from excitatory to inhibitory due to variations in the intracellular $Cl^-$ concentration during development. From these observations, we have discussed the developmental shift in the receptor activation of taurine-sensitive chloride channels in neurons of the postnatal cerebral cortex.

## METHODS

### Animals

Pregnant or postnatal Institute of Cancer Research (ICR) mice were purchased from Sankyo Laboratory Service (Tokyo, Japan). The day of birth was defined as postnatal day 0 (P0). All experiments were carried out in accordance with the guidelines for Animal Experiments of the Graduate School of Frontier Sciences, The University of Tokyo.

### Preparation of Acute Living Slices

ICR mice were deeply anaesthetized by hypothermia (early developmental stage (P2–P5) or ethyl ether (in excess of P6), respectively, prior to decapitation. Brains were then quickly removed and placed in ice-cold low-$Ca^{2+}$ artificial cerebrospinal fluid (ACSF) (composition in mM: 124 NaCl, 26 $NaHCO_3$, 2.5 KCl, 10 glucose, 4.5 $MgCl_2$, 0.1 $CaCl_2$) pregassed with 95% $O_2$ and 5% $CO_2$ (pH 7.4). For preparation of brain slices, brains were glued to the cutting stage of a vibrating slice cutter (DTK-1000; Dosaka, Kyoto, Japan), rostral side up, and sliced into coronal sections (400 $\mu$m) that included the somatosensory cortex. The slices were incubated at 37°C for 30 min (recovery period) in oxygenated standard ACSF (composition in mM: 124 NaCl, 26 $NaHCO_3$, 2.5 KCl, 10 glucose, 1 $MgCl_2$, 2 $CaCl_2$), then maintained at room temperature during subsequent experiments.

### Patch-Clamp Recording

Slices were fixed by nylon thread to a U-shaped platinum frame and then positioned in a recording chamber (volume approximately 0.2 ml, RC-26GLP; Warner Instruments, Hamden, CT) and submerged in and superfused with oxygenated standard ACSF at a flow rate of 1–2 ml/min as described before (Fukuda et al., 2003). The slices were observed with the aid of a microscope (BX-50WI; Olympus, Tokyo, Japan), with images recorded from the light port using a chilled charge-coupled device (CCD) video camera (C5985; Hamamatsu Photonics, Hamamatsu, Japan). Patch pipettes with resistances of 5–8 MΩ were made from fire-polished borosilicate capillary glass of 1.2 mm outer diameter (1B120F-2; World Precision Instruments, Sarasota, FL), using a programmable vertical puller (P-87; Sutter Instruments, Novato, CA). The pipette solution for whole-cell patch-clamp recordings contained (mM): 140 CsCl, 1 $CaCl_2$, 2 MgATP, 0.3 NaGTP, 10 EGTA, 10 HEPES (adjusted to pH 7.2 with CsOH).

The pipette solution for gramicidin perforated patch recording contained (in mM): 130 KCl, 5 NaCl, 0.4 $CaCl_2$, 1 $MgCl_2$, 10 HEPES, 1.1 EGTA, and was adjusted to pH 7.2 with KOH. Gramicidin (Sigma, St. Louis, MO) was first dissolved in dimethylsulfoxide (DMSO) (Sigma) to prepare a stock solution of 2 g/L and then diluted in the pipette solution to a final concentration of 5 mg/L. Fresh gramicidin-containing solutions were prepared every 2 h. After establishment of the cell-attached configuration (1–10 GΩ seal resistance), the whole-cell mode was established with negative pressure and negative current pulses using a CEZ-2400 amplifier (Nihon-Kohden, Tokyo, Japan). Perforated patch recordings were obtained using identical methods, except that mechanical rupture of the membrane was omitted. The progress of perforation was evaluated by monitoring the decrease in the membrane resistance (Owens et al., 1996).

Recordings were started after the membrane resistance had stabilized; usually 10–15 min after the high-resistance seal had been established. During the recordings, the membrane holding potential was set to −60∼−70 mV. Data were recorded at room temperature with a CEZ-2400 amplifier. The membrane current was sampled on-line at 4 kHz (PowerLab; AD Instruments, Grand Junction, CO) after filtering at 2 kHz. Signals were recorded with Chart 4.0 software (AD Instruments) and stored on the hard disk of a

personal computer for later off-line analysis with Igor Pro 4.01 software (WaveMatrics, Lake Oswego, OR).

## Drug Application

In some experiments, agonists were applied to one particular neuron using a "Y-tube" system (Greenfield and Macdonald, 1996; also kindly instructed by Dr. Nabekura, Kyushu University). In all other cases, agonists were pressure-applied locally using a PicoPump (PV820; World Precision Instruments) via a glass pipette positioned about 50 μm from the soma of the recorded cell. Antagonists were bath-applied in all experiments.

## Patch-Clamp Data Analyses

***Dose-Response Curves.*** Dose-response relationships for taurine were fitted to the Hill equation as follows:

$$I = I_{max}/1 + (EC_{50}/[\text{taurine}]^n)$$

where $I$ is the peak current measured for a given taurine concentration, $I_{max}$ the current at the maximal taurine concentration, $EC_{50}$ the concentration of taurine required for a half-maximal response, and $n$ the Hill coefficient (slope factor). Analysis of dose-response relationships was carried out using Origin 7.0 software (Demo) (OriginLab, Northampton, MA).

***Calculation of $E_{Cl}$ and the Intracellular $Cl^-$ Concentration ($[Cl^-]_i$).*** To calculate the equivalent potential of ion A, the Nernst equation is employed:

$$E_A = \frac{RT}{FZ} \ln \frac{[A]_o}{[A]_i}$$

where $R$ is the thermodynamic gas constant (8.31 J/mol/K), $T$ the absolute temperature, $F$ the Faraday Constant (96,500 C/mol), $Z$ the valence of the ion (in the case of $Cl^-$, $-1$), and $[A]_o$ and $[A]_i$ the outside and inside concentration of ion A, respectively. In this study, I–V data were fitted by a line, with the resulting Y-intercept defined as $E_{Cl}$. $[Cl^-]_i$ was calculated by substituting the value of $E_{Cl}$, as well as 300 K for $T$, $-1$ for $Z$, and 133.5 mM for $[Cl^-]_o$ (ACSF composition) to the Nernst equation.

## Immunocytochemistry

Mouse brains at P5 and P33 were fixed by transcardial perfusion with phosphate-buffered saline (PBS; in mM: 137 NaCl, 8.1 $Na_2PO_4$, 2.68 KCl, 1.47 $KH_2PO_4$), followed by 4% paraformaldehyde in PBS. In each case, the brain was removed and post-fixed with 4% paraformaldehyde at 4°C overnight, followed by treatment in 30% sucrose in Tris-buffered saline (TBS; in mM: 137 NaCl, 2.68 KCl, 25 Tris) overnight. Post-fixed brains were embedded in Optimal Cutting Temperature (O.C.T.) compound (Sakura, Tokyo, Japan) and frozen at −80°C (Okada et al., 2003). Frozen blocks were sliced into 40 μm-thick sections using a cryostat (MICRON, Walldorf, Germany), and then preserved in cryoprotectant solution (30% ethylene glycol and 30% glycerol in 0.05 M phosphate buffer) at −20°C. Thereafter, sections were first placed in TBS for 10 min to wash out the cryoprotectant and then blocked with blocking buffer [5% normal goat serum (NGS) in 0.3% Triton-TBS] for 30–60 min at room temperature. Free-floating sections were incubated for 3 days at 4°C with monoclonal anti-glycine receptor (mouse IgG; 1:100 dilution; Alexis, Lausen, Switzerland) and anti-sodium, potassium, chloride cotranporter 1 (NKCC1) (Plotkin et al., 1997) (rabbit IgG; 1:100 dilution; Chemicon, Temecula, CA) in modified blocking solution (5% NGS in 0.1% Triton-TBS). After three washings in TBS (10, 15, and 15 min), sections were incubated with fluorochromo-conjugated secondary antibodies, Alexa 488 (anti-rabbit IgG; 1:1000 dilution, Molecular Probes, Eugene, OR) and RRX (anti-mouse IgG; 1:200 dilution; Jackson Immunoresearch, West Grove, PA), dissolved in the modified blocking solution at room temperature for 2 h, and then washed in TBS. The stained sections were aligned on glass slides and incubated for 10 min in 4′,6-diamidino-2-phenylindole (DAPI) (1:1000 dilution; Sigma) dissolved in 0.1% Triton-TBS, and then sealed by Immu-mount (Shandon, Pittsburgh, PA) with 2% 1,4-diazabicyclo[2.2.2]octane (DABCO) (Sigma). Stained sections were analyzed with a confocal microscope (TCS SP2; Leica, Mannheim, Germany) (Koketsu et al. 2003).

# RESULTS

## Response of Cortical Neurons to Taurine during the Postnatal Stages

Taurine-induced currents in supragranular layer neurons (layers II–IV) were measured by means of whole-cell patch-clamp recordings. Figure 1(A) shows that current activation in a P6 neuron occurred when taurine was employed at a concentration in excess of 0.3 mM. In general, while no evidence of desensitization was observed in P2–7 neurons for taurine concentrations up to 1 mM, slight desensitization was observed at concentrations above 1 mM. Currents were clearly desensitized at taurine concentrations in excess of 3 mM. Average dose-response values for five P2–7 neurons were fitted by a Hill equation, for which the calculated half-maximal concentration ($EC_{50}$) and Hill coefficient were 7.7 mM and 0.94, respectively [Fig. 1(B)]. Recorded neurons in the supragranular layer which stained with lucifer yellow possessed apical dendrites and seemed to be typical of pyramidal neurons [Fig. 1(C)].

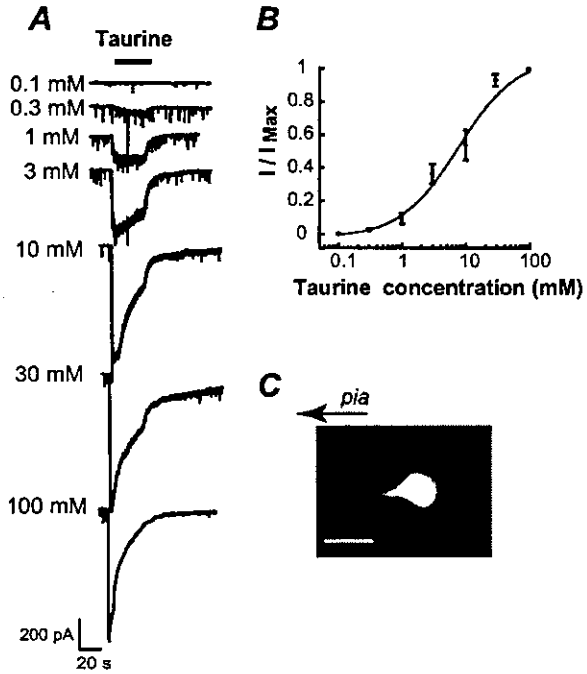


**Figure 1** Responses of early developmental stage (P6) neurons to activation by taurine. (A) Currents measured in a P6 neocortical neuron in response to exposure to different concentrations of taurine. Recordings made in whole-cell patch-clamp mode. Note that at lower concentrations (~1 mM) taurine evoked electrical responses without desensitization. Comparable results were obtained from four other neurons and their recording data were utilized for subsequent analysis. (B) Dose-response curve for taurine in early developmental stage (P2–7) from the recordings of five neurons, which were obtained from five brain slices of three mice. The data were fitted by a Hill equation for which the $EC_{50}$ and Hill coefficient were 7.7 mM and 0.94, respectively. (C) Representative morphology of a neuron typical of one from which recordings were made, visualized here by lucifer yellow staining. Scale bar: 20 $\mu$m.

Responses of cortical neurons to taurine were further analyzed for later developmental stages. As shown in Figure 2, taurine triggered currents in P27–36 neocortical neurons. Average dose-response values for four P30 neurons were fitted by a Hill equation, for which the calculated half-maximal concentration ($EC_{50}$) and Hill coefficient were 3.9 mM and 0.95, respectively [Fig. 2(B)]. The morphology of recorded neurons was visualized with the aid of lucifer yellow injection; an example of one of these neurons is shown in Figure 2(C) which exhibits several processes and pyramidal morphology. Cortical neurons at a more developed stage, such as in young adults, were also tested for taurine-evoked responses. As shown in Figure 3, taurine evokes currents in cortical neurons from 8-week-old mice at concentrations as low as 0.3 mM. This is the first demonstration, to our knowledge, of taurine triggering an electrical response in adult cortical neurons, and implies that taurine could act as a neuromodulator in the adult cerebral cortex.

## Developmental Shift of Taurine-Sensitive Receptor Channels from GlyR to $GABA_AR$

The current response triggered by taurine application was subsequently examined in neurons from two developmental stages: the early developmental stage (P2–7) and the late developmental stage (P27–36). In order to analyze the properties of the receptor-coupled channels via which the taurine-evoked currents were conducted, pharmacological agents were subsequently used to inhibit receptors thought to be involved in the mechanism.

As mentioned in the Introduction, it has been reported that taurine acts as an agonist for glycine receptors (Flint et al., 1998; Mori et al., 2002) and $GABA_A$ receptors (Puopolo et al., 1998; del Olmo et al., 2000). On this basis, we evaluated the properties of taurine responses and the taurine-induced activation of glycine receptors and/or $GABA_A$ receptors in cortical neurons from mouse neocortex from each of the developmental stages.

To identify the receptor-coupled channels mediating these currents, specific receptor antagonists were used in whole-cell patch-clamp recordings. As shown in Figure 4, the currents evoked in a P5 neuron by taurine application (2 mM) were mostly blocked by strychnine, a selective antagonist of glycine receptors. The remaining small residual current was completely blocked by the addition of bicuculline methiodide (BMI), a selective antagonist of $GABA_A$ receptors. In control experiments, it was confirmed that the strychnine dosage used—3 $\mu$M—completely inhibited the glycine response but did not disturb the GABA response, and similarly that the BMI dose used (100 $\mu$M) completely blocked the GABA response. Although taurine activated $GABA_A$ receptors as well as glycine receptors in this P5 neuron, the response was largely mediated by glycine receptors.

In cortical neurons from the late developmental stage (P27–36), the taurine response was only partially inhibited by strychnine, with the remainder completely inhibited by the addition of bicuculline methiodide (Fig. 5). Table 1 summarizes the results obtained from neurons in the early and late developmental stages. The component that was inhibited by the application of strychnine is defined as "GlyR," and the residual component, which is completely in-

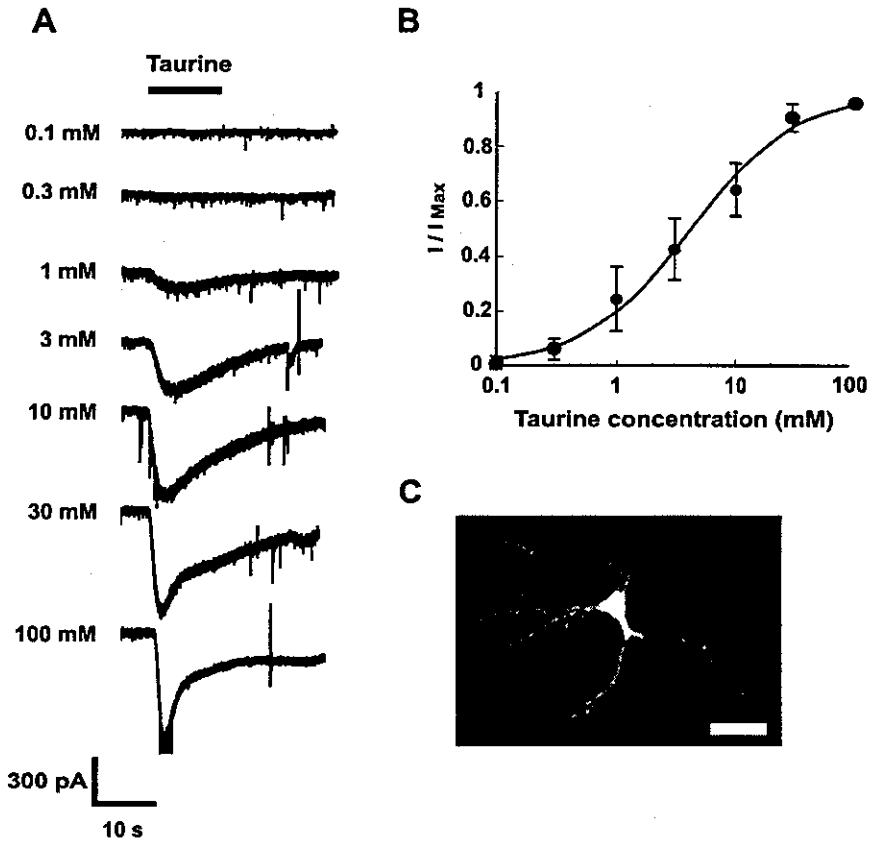


**Figure 2** Responses of late developmental stage (P30) neurons to activation by taurine. (A) Currents measured in a P30 neocortical neuron in response to exposure to different concentrations of taurine. Recordings made in whole-cell patch-clamp mode. Comparable results were obtained from three other neurons and their recording data were utilized for subsequent analysis. (B) Dose-response curve for taurine in a late developmental stage (P30) from the recordings of four neurons, which were obtained from three brain slices of three mice. The data were fitted by a Hill equation for which the $EC_{50}$ and Hill coefficient were 3.9 mM and 0.95, respectively. (C) Representative morphology of a neuron typical of one from which recordings were made, visualized here by lucifer yellow staining. Scale bar: 20 $\mu$m.

hibited by the additional application of bicuculline methiodide, is defined as "$GABA_AR$." The average taurine response evoked in the absence of any inhibitor for cells at each developmental stage was designated as the 100% value, and each component (GlyR or $GABA_AR$) then normalized to this value. The results clearly show a developmental shift in the taurine target, from the glycine receptor to the $GABA_A$ receptors.

## Developmental Stages Determine the Physiological Functions of Taurine

We studied the physiological effects of taurine on the taurine-sensitive receptor channels. Given that taurine acts on $Cl^-$ ion channels, the gramicidin perforated patch-clamp method was employed to monitor the physiological action of taurine in maintaining the intracellular $Cl^-$ concentration. The effects of taurine application were observed both in the early and later developmental stages (Fig. 6). These observations were carried out under current-clamp mode, in which changes in membrane potential could be recorded in response to exposure of cortical neurons to taurine. For neurons in the early developmental stage (P2), taurine application induced a +15 mV depolarization, from −70 mV to −55 mV [Fig. 6(A)]. I–V curves were constructed by switching from current-clamp to voltage-clamp mode and then measuring current amplitudes in response to changes in holding potentials. The equilibrium potential for taurine for the neuron whose experimental results are shown in Figure 6(A) was thus found to be −42 mV, from which the intracellular $Cl^-$ concentration was calculated from the

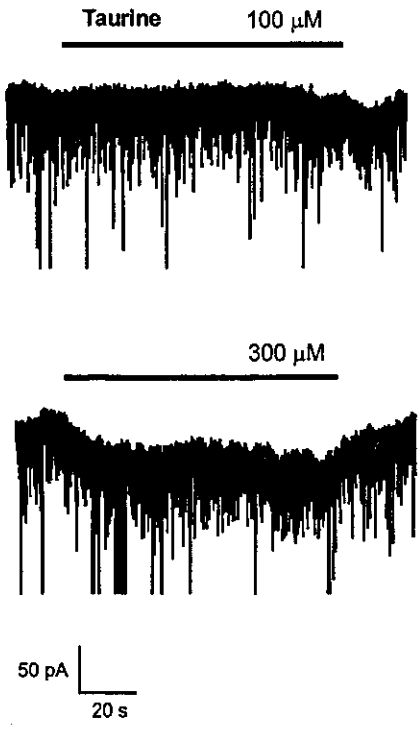


**Figure 3** Electrical responses of adult neocortical neurons. Taurine evoked responses in adult neocortical neurons (8-week-old mice) when used at a concentration of 0.3 mM. Comparable results were obtained from three other adult neurons, from three brain slices of three mice.

Nernst equation to be 26.2 mM. Since taurine-evoked currents were completely inhibited by the $Cl^-$ channel receptor antagonists strychnine and BMI (Fig. 4), the equilibrium potential for taurine (see comments above) was considered to be equal to that for $Cl^-$. For a neuron from the later developmental stage (P33), similar experiments were performed [Fig. 6(B)]. In this case, the membrane potential hyperpolarized by $-4$ mV (from $-73$ mV to $-77$ mV) in response to taurine application, which gave rise to an equilibrium potential of $-86.8$ mV and an intracellular $Cl^-$ concentration of 4.62 mM.

Following on from these results, the change of intracellular $Cl^-$ concentrations was examined for three different developmental stages (Fig. 7). Results showed a decrease of intracellular $Cl^-$ concentration as the postnatal period progressed. We considered that the decrease in the intracellular $Cl^-$ concentration measured in older cortical neurons could be associated with a decrease in the density of the $Na^+$-K-$2Cl^-$ cotransporter, NKCC1. An anti-NKCC1 antibody was thus used to enable immunohistochemical examination of the expression of this cotransporter in cortical neurons at the various developmental stages. The expression of GlyRs in developing cortical neurons was also evaluated. In neocortical neurons from animals at an early developmental stage (P5), glycine receptors were found to be densely co-expressed with NKCC1 in most cells of the neocortical layer II/III (Fig. 8). In neurons from animals at a later developmental stage (P33), cells were present in relatively sparse amounts in the cortical plate as revealed by DAPI staining, but many of the cells stained positively for the glycine

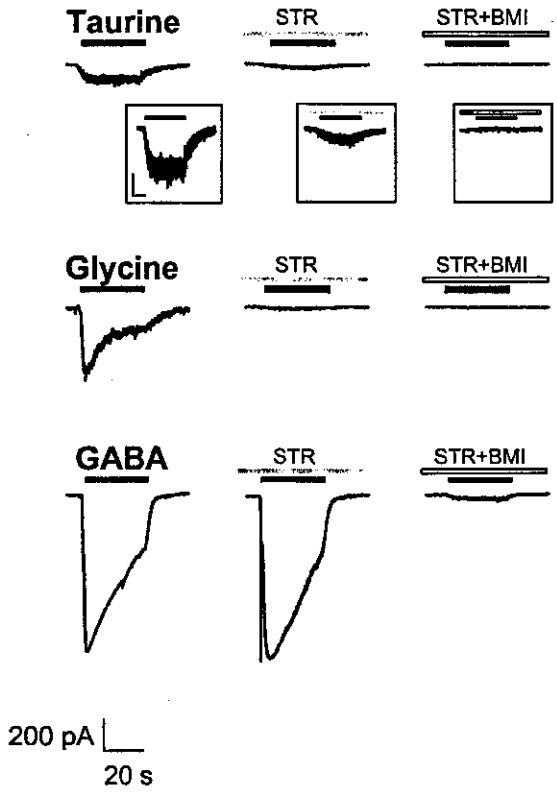


**Figure 4** Effects of glycine receptor and $GABA_A$ receptor antagonists on taurine-evoked current responses in a P5 neocortical neuron. Taurine (2 mM) evokes an electrical response in a layer II/III P5 neuron. Solid bar indicates the time of taurine application. Insets show magnifications of the taurine responses. Scale bars in insets are 50 pA and 10 s. The taurine response (upper trace) was mostly inhibited by the application of strychnine (STR; 3 μM). Longer bar shows the time of inhibitor application. The residual current elicited during the taurine application was completely blocked by the addition of bicuculline methiodide (BMI; 100 μM). Middle trace shows a control experiment where the same neuron as in upper trace is activated by glycine (1 mM). This response was completely blocked by STR. The lower trace shows a control experiment, again on the same neuron, with activation by GABA (100 μM). On this occasion, the response was blocked by BMI (100 μM). These control experiments highlight the specificity of the inhibitors used in this study. Comparable results were obtained from 10 other neurons, and these recording data were utilized in Table 1.

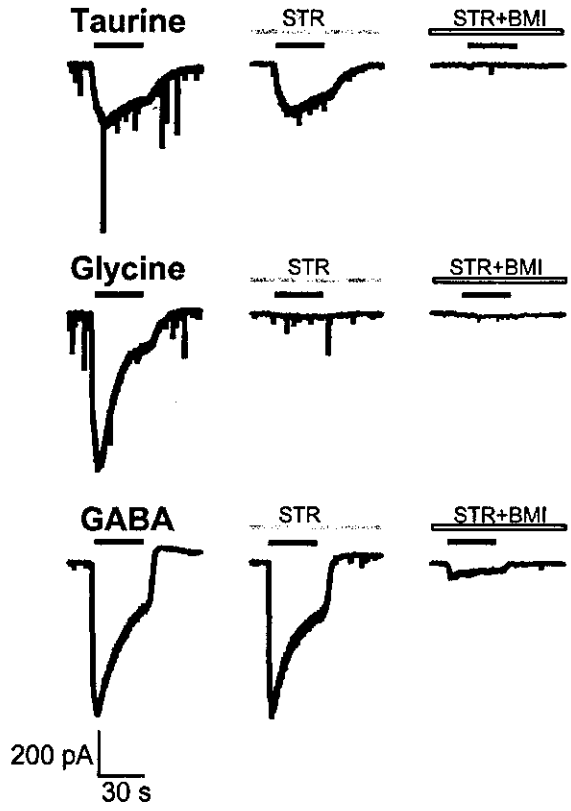


**Figure 5** Effects of glycine receptor and $GABA_A$ receptor antagonists on taurine-evoked current responses in a P33 neocortical neuron. Taurine (2 mM), glycine (1 mM), and GABA (100 $\mu$M) were applied to a P33 neuron in neocortical layer II/III. Experimental conditions are the same as those described in the legend to Figure 4 . The effect of STR is less than that seen for the P5 neuron in Figure 4 . Comparable results were obtained from two other neurons, and these recording data were utilized in Table 1.

receptor (Fig. 8). NKCC1 was negatively stained in the whole slice, meaning that the co-expression of glycine receptors and NKCC1 was not observed in

**Table 1 Principal Target of Taurine Shifts from Glycine Receptors to $GABA_A$ Receptors as Development Proceeds**[1]

| Developmental Stage | GlyR (%) | $GABA_AR$ (%) |
|---|---|---|
| Early stage | 82.2 | 17.8 |
| Late stage | 27.6 | 72.4 |

[1] Early developmental stage (early stage), P2–7 ($n$ = 11, from 11 slices of five mice); late developmental stage (late stage), P27–36 ($n$ = 3, from three slices of two mice). The current component that was inhibited by strychnine (3 $\mu$M) was defined as the "GlyR" component of the current, with the residual current defined as the "$GABA_AR$" component. The percentages of GlyR and $GABA_AR$ are the mean values. S.E.M. of the value at each stage was 4.1% (early stage) and 4.5% (late stage).

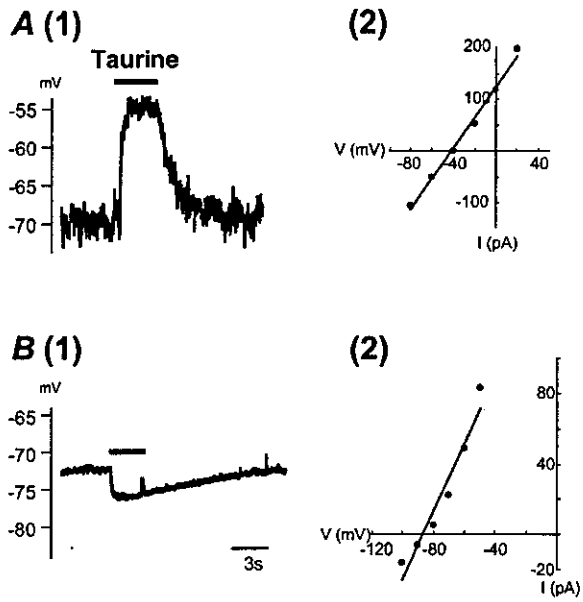


**Figure 6** Two different effects of taurine as a function of developmental stage. (A) (1) Gramicidin perforated patch-clamp recording in current-clamp mode from a P2 neocortical neuron demonstrates that taurine application (10 mM) induces membrane depolarization. (2) For this neuron, $E_{Cl}$ = −42.0 mV and $[Cl^-]_i$ = 26.2 mM as calculated by the Nernst Equation. (B) (1) Recording from a P33 neuron shows cell membrane hyperpolarization upon taurine application. (2) In this neuron, $E_{Cl}$ = −86.8 mV and $[Cl^-]_i$ = 4.62 mM.

P33 neocortical layer II/III neurons. It can therefore be stated that the expression of NKCC1 in neurons in these experiments was limited to the early developmental stage (P2–7), which is consistent with the presence of a developmental program for regulating the intracellular $Cl^-$ concentration in mammalian cortical neurons.

## DISCUSSION

In this communication, we clearly demonstrate that taurine activates specific chloride channels in developing cortical neurons in a manner dependent on the postnatal stage of the developing brain (from P0–P36 ). The physiological effect of activation of the taurine-receptor channels changes from excitatory to inhibitory over the course of postnatal development due to the marked decrease in the intracellular $Cl^-$ concentration during this time. This developmental shift occurs in parallel with the shift in the receptor-type responsible for mediating the activation by taurine, from glycine receptors to $GABA_A$ receptors. In addition, it has been re-

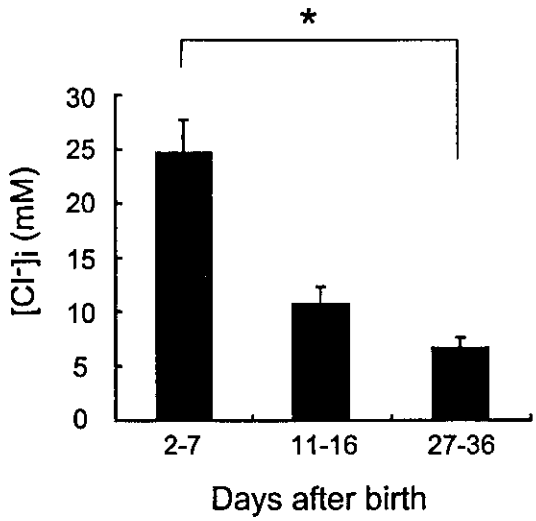


**Figure 7** Decrease in intracellular $Cl^-$ concentration during development. $[Cl^-]_i$ was estimated by means of gramicidin perforated patch-clamp recordings in developing neocortical layer II/III neurons. Numbers of trials: early stage (P2–7), $n = 35$; intermediate stage (P11–15), $n = 8$; late stage (P27–36), $n = 3$. Values are given as means ± S.E.M. $^*p < 0.05$, Student's $t$-test for unpaired samples.

ported that a gradual decrease in brain taurine concentration from birth is completed by the time of weaning or thereabouts in rodents and primates (Sturman, 1986). From these results, we can postulate the existence of genetically programmed, bidirectional functions of taurine in the developing cerebral cortex: at the early postnatal stage, taurine would function as a promoter of cortical circuit formation, whereas later on in postnatal development, taurine assumes the role of toning down the hyperexcitable behavior of immature cortical circuitry.

Cortical circuit formation is strictly regulated as a function of postnatal age (Feldman et al., 1999). Remarkably, thalamocortical long-term potentiation (LTP) is only observed in brain slices from P7 animals or younger (Crair and Malenka, 1995). This developmental time course is similar to the critical period for experience-dependent plasticity of thalamocortical synapses in vivo (Schlaggar et al., 1993). This critical period occurs in synchrony with the early postnatal stage (P0–P6), when the interaction between taurine and glycine receptors serves as an inducer for NMDA receptor activation by overriding the effects of voltage-dependent $Mg^{2+}$ block (Flint et al., 1998; Miyakawa et al., 2002).

The expression of glycine receptors in cortical neurons has been reported in a series of studies. In neonates, $\alpha 2$ subunits and $\beta$ subunits are expressed in cortical neurons in developing cortical plates (Malosio et al., 1991). It has been also reported that glycine receptors in neonates consist of five $\alpha 2$ subunits, expressed as a homopentamer (Langosch et al., 1988; Takahashi et al., 1992; Flint et al., 1998). In relation to later developmental stages, little information is available concerning glycine receptor expression in the neocortex. In this study, we have demonstrated for the first time, to our knowledge, the expression of glycine receptors in cortical neurons, even though at this stage taurine preferentially activates $GABA_A$ receptors rather than glycine receptors. This developmental shift in the target of taurine probably stems from a developmental shift in the subunit compositions of glycine and $GABA_A$ receptors.

We have shown, in this communication, that a taurine-induced opening of chloride channels leads to a decrease in membrane potential of neurons after the later developmental period. It has also been reported that excitotoxic amino acids such as glutamate signif-

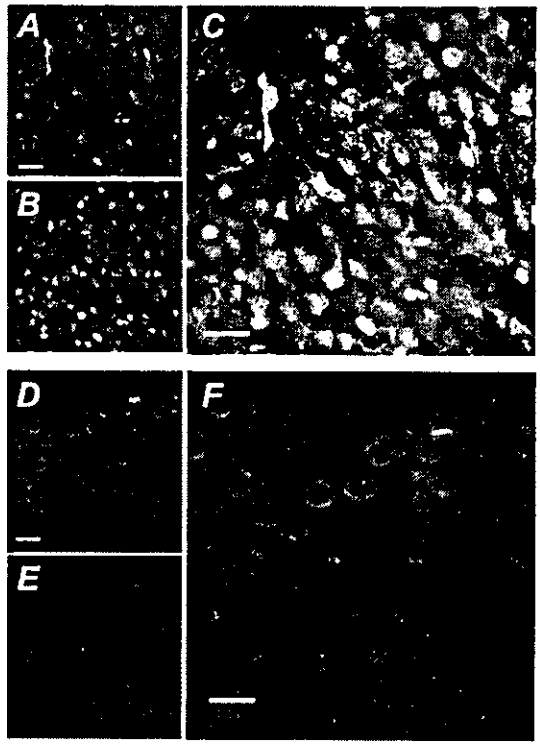


**Figure 8** Expression of glycine receptors and NKCC1 in layer II/III cortical neurons of early (P5) and late (P33) developmental stages. (A–C) Images from P5 neurons. Glycine receptors (A) and $Na^+$-$K^+$-$2Cl^-$ cotransporters (NKCC1; B) were densely co-expressed in P5 neocortical neurons. (C) Merged image of A and B. (D–F) Images from P33 neurons. Glycine receptors (D) were expressed at the surface of P33 cortical neurons, but no NKCC1 expression was observed (E). (F) Merged image of A and B with DAPI staining for identification of cortical cells. Scale bars: 20 $\mu$m.

icantly stimulate the release of taurine (Saransaari and Oja, 1997; Oja and Saransaari, 2000). It is conceivable that taurine at this stage could contribute to a reduction in the membrane hyperexcitability of neuronal cortical circuitry. Indeed, GABA as the principal inhibitory neurotransmitter in the neocortex plays an important role in epilepsy (Treiman, 2001). Since the kinetics of the taurine response on $GABA_A$ receptors are quite unique when compared to the primary ligand GABA (Ye et al., 1997; del Olmo et al., 2000), taurine could therefore be able to act as a secondary ligand for $GABA_AR$ in the mammalian cerebral cortex, serving as an additional safeguard against hyperexcitability in later postnatal stages of developing cerebral cortex.

We thank Drs. Fusao Kato and Junichi Nabekura for informative discussions.

## REFERENCES

Ben-Ari Y, Cherubini E, Corradetti R, Gaiarsa JL. 1989. Giant synaptic potentials in immature rat CA3 hippocampal neurones. J Physiol (Lond) 416:303–325.

Ben-Ari Y, Khazipov R, Leinekugel X, Caillard O, Gaiarsa JL. 1997. GABAA, NMDA and AMPA receptors: a developmentally regulated 'menage a trois'. Trends Neurosci 20:523–529.

Chesney RW. 1985. Taurine: its biological role and clinical implications. Adv Pediatr 32:1–42.

Crair MC, Malenka RC. 1995. A critical period for long-term potentiation at thalamocortical synapses. Nature 375:325–328.

del Olmo N, Bustamante J, del Rio RM, Solis JM. 2000. Taurine activates GABA(A) but not GABA(B) receptors in rat hippocampal CA1 area. Brain Res 864:298–307.

Feldman DE, Nicoll RA, Malenka RC. 1999. Synaptic plasticity at thalamocortical synapses in developing rat somatosensory cortex: LTP, LTD, and silent synapses. J Neurobiol 41:92–101.

Flint AC, Liu X, Kriegstein AR. 1998. Nonsynaptic glycine receptor activation during early neocortical development. Neuron 20:43–53.

Fukuda S, Kato F, Tozuka Y, Yamaguchi M, Miyamoto Y, Hisatsune T. 2003. Two distinct subpopulations of nestin-positive cells in adult mouse dentate gyrus. J Neurosci 23:9357–9366.

Greenfield LJ Jr, Macdonald RL. 1996. Whole-cell and single-channel alpha1 beta1 gamma2S GABAA receptor currents elicited by a "multipuffer" drug application device. Pflugers Arch 432:1080–1090.

Huxtable RJ. 1989. Taurine in the central nervous system and the mammalian actions of taurine. Prog Neurobiol 32:471–533.

Isaac JT, Crair MC, Nicoll RA, Malenka RC. 1997. Silent synapses during development of thalamocortical inputs. Neuron 18:269–280.

Koketsu D, Mikami A, Miyamoto Y, Hisatsune T. 2003. Non-renewal of neurons in the cerebral neocortex of adult Macaque monkeys. J Neurosci 23:937–942.

Kontro P, Oja SS. 1987a. Co-operativity in sodium-independent taurine binding to brain membranes in the mouse. Neuroscience 23:567–570.

Kontro P, Oja SS. 1987b. Glycinergic systems in the brain stem of developing and adult mice: effects of taurine. Int J Dev Neurosci 5:461–470.

Langosch D, Thomas L, Betz H. 1988. Conserved quaternary structure of ligand-gated ion channels: the postsynaptic glycine receptor is a pentamer. Proc Natl Acad Sci USA 85:7394–7398.

Liao D, Hessler NA, Malinow R. 1995. Activation of postsynaptically silent synapses during pairing-induced LTP in CA1 region of hippocampal slice. Nature 375: 400–404.

Linne ML, Jalonen TO, Saransaari P, Oja SS. 1996. Taurine-induced single-channel currents in cultured rat cerebellar granule cells. Adv Exp Med Biol 403:455–462.

Malminen O, Kontro P. 1986. Modulation of the GABA-benzodiazepine receptor complex by taurine in rat brain membranes. Neurochem Res 11:85–94.

Malminen O, Kontro P. 1987. Actions of taurine on the GABA-benzodiazepine receptor complex solubilized from rat-brain. Neurochem Int 11:113–117.

Malosio ML, Marqueze-Pouey B, Kuhse J, Betz H. 1991. Widespread expression of glycine receptor subunit mRNAs in the adult and developing rat brain. EMBO J 10:2401–2409.

Miyakawa N, Uchino S, Yamashita T, Okada H, Nakamura T, Kaminogawa S, Miyamoto Y, Hisatsune T. 2002. A glycine receptor antagonist, strychnine, blocked NMDA receptor activation in the neonatal mouse neocortex. Neuroreport 13:1667–1673.

Mori M, Gahwiler BH, Gerber U. 2002. Beta-alanine and taurine as endogenous agonists at glycine receptors in rat hippocampus in vitro. J Physiol 539:191–200.

Oja SS, Saransaari P. 2000. Modulation of taurine release by glutamate receptors and nitric oxide. Prog Neurobiol 62:407–425.

Okada H, Miyakawa N, Mori, H, Mishina M, Miyamoto Y, Hisatsune T. 2003. NMDA receptors in cortical development are essential for the generation of coordinated increases in [Ca2+]i in 'neuronal domains'. Cereb Cortex 13:749–757.

Owens DF, Boyce LH, Davis MB, Kriegstein AR. 1996. Excitatory GABA responses in embryonic and neonatal cortical slices demonstrated by gramicidin perforated-patch recordings and calcium imaging. J Neurosci 16: 6414–6423.

Plotkin MD, Snyder EY, Hebert SC, Delpire E. 1997. Expression of the Na-K-2Cl cotransporter is developmentally regulated in postnatal rat brains: a possible mechanism underlying GABA's excitatory role in immature brain. J Neurobiol 33:781–795.

Puopolo M, Kratskin I, Belluzzi O. 1998. Direct inhibitory effect of taurine on relay neurones of the rat olfactory bulb in vitro. Neuroreport 9:2319–2323.

Saransaari P, Oja SS. 1997. Taurine release from the developing and ageing hippocampus: stimulation by agonists of ionotropic glutamate receptors. Mech Ageing Dev 99:219–232.

Schlaggar BL, Fox K, O'Leary DDM. 1993. Postsynaptic control of plasticity in developing cortex. Nature 364: 623–626.

Sturman JA. 1981. Origin of taurine in developing rat brain. Brain Res 254:111–128.

Sturman JA. 1986. Nutritional taurine and central nervous system development. Ann NY Acad Sci 477:196–213.

Sturman JA, Rassin DK, Gaull GE. 1977. Taurine in developing rat brain: transfer of [$^{35}$S] taurine to pups via the milk. Pediatr Res 11:28–33.

Takahashi T, Momiyama A, Hirai K, Hishinuma F, Akagi H. 1992. Functional correlation of fetal and adult forms of glycine receptors with developmental changes in inhibitory synaptic receptor channels. Neuron 9:1155–1161.

Treiman DM. 2001. GABAergic mechanisms in epilepsy. Epilepsia 42:8–12.

Ye G, Tse ACO, Yung W. 1997. Taurine inhibits rat substantia nigra pars reticulate neurons by activation of GABA- and glycine-linked chloride conductance. Brain Res 749:175–179.

 Related Commentary, page 23

# Dopaminergic neurons generated from monkey embryonic stem cells function in a Parkinson primate model

Yasushi Takagi,[1,2] Jun Takahashi,[1] Hidemoto Saiki,[3] Asuka Morizane,[1] Takuya Hayashi,[4] Yo Kishi,[1] Hitoshi Fukuda,[1] Yo Okamoto,[1] Masaomi Koyanagi,[1] Makoto Ideguchi,[1] Hideki Hayashi,[1] Takayuki Imazato,[1] Hiroshi Kawasaki,[5] Hirofumi Suemori,[6] Shigeki Omachi,[7] Hidehiko Iida,[4] Nobuyuki Itoh,[7] Norio Nakatsuji,[6] Yoshiki Sasai,[2,5] and Nobuo Hashimoto[1]

[1]Department of Neurosurgery, Kyoto University Graduate School of Medicine, Kyoto, Japan. [2]Organogenesis and Neurogenesis Group, Center for Developmental Biology, RIKEN, Kobe, Japan. [3]Department of Neurology, Kyoto University Graduate School of Medicine, Kyoto, Japan. [4]Department of Experimental Radiology, National Cardiovascular Center, Osaka, Japan. [5]Department of Medical Embryology and Neurobiology and [6]Department of Development and Differentiation, Institute for Frontier Medical Sciences, Kyoto University, Kyoto, Japan. [7]Department of Genetic Biochemistry, Kyoto University Graduate School of Pharmaceutical Sciences, Kyoto, Japan.

**Parkinson disease (PD) is a neurodegenerative disorder characterized by loss of midbrain dopaminergic (DA) neurons. ES cells are currently the most promising donor cell source for cell-replacement therapy in PD. We previously described a strong neuralizing activity present on the surface of stromal cells, named stromal cell–derived inducing activity (SDIA). In this study, we generated neurospheres composed of neural progenitors from monkey ES cells, which are capable of producing large numbers of DA neurons. We demonstrated that FGF20, preferentially expressed in the substantia nigra, acts synergistically with FGF2 to increase the number of DA neurons in ES cell–derived neurospheres. We also analyzed the effect of transplantation of DA neurons generated from monkey ES cells into 1-methyl-4-phenyl-1,2,3,6-tetrahydropyridine–treated (MPTP-treated) monkeys, a primate model for PD. Behavioral studies and functional imaging revealed that the transplanted cells functioned as DA neurons and attenuated MPTP-induced neurological symptoms.**

## Introduction

Parkinson disease (PD) is a neurodegenerative disorder characterized by the loss of midbrain dopaminergic (DA) neurons, with subsequent reductions in striatal dopamine levels. While initial pharmacological treatment with L-dihydroxyphenylalanin (L-DOPA) can attenuate symptoms, the efficacy of this treatment gradually decreases over time. The development of motor complications then requires additional treatments, including deep brain stimulation and fetal DA neuron transplantation (1–3). Both studies of animal models and clinical investigations have shown that transplantation of fetal DA neurons can produce symptomatic relief (4–8). The technical and ethical difficulties in obtaining sufficient and appropriate donor fetal brain tissue, however, have limited the application of this therapy.

ES cells are self-renewing, pluripotent cells derived from the inner cell mass of the preimplantation blastocyst. These cells have many of the characteristics required of a cell source for cell-replacement therapy, including proliferation and differentiation capacities (9). We previously discovered that a strong neuralizing activity, which we called stromal cell–derived inducing activity (SDIA), is present on the surface of stromal cells. In the absence of exogenous bone morphogenic protein-4, mouse ES cells differentiate efficiently into neural precursors and neurons when cultured for 1 week on SDIA-expressing mouse stromal cells (PA6 cells) (10). Recently, SDIA induction has also been applied to primate ES cells, which generated large numbers of neural precursors and postmitotic neurons when cultured on PA6 cells for two weeks (11). The SDIA method is both technically simple and efficient, producing significant numbers of midbrain DA neurons (10, 11).

Self-renewing, multipotent neural progenitors can be cultured as neurospheres (12). In this study, we generated neural progenitors from monkey ES cells, then expanded them as neurospheres, which contained progenitors of DA neurons. In addition, we analyzed the effect of FGF20, a novel member of the FGF family of growth factors that is expressed exclusively in the substantia nigra of the brain and is reported to have a protective effect on DA neurons (13). We observed increased DA neuron induction following treatment with FGF20. Furthermore, we transplanted neurons generated by this method into 1-methyl-4-phenyl-1,2,3,6-tetrahydropyridine–treated (MPTP-treated) cynomolgus monkeys, a primate model for PD. We found that transplanted cells were able to function as DA neurons and could diminish Parkinsonian symptoms. This is the first report, to our knowledge, demonstrating the efficacy of transplantation therapy using ES cell–derived DA neurons in an experimental primate model of PD.

## Results

*Induction of neural progenitors from monkey ES cells.* To enrich graftable neural progenitors, we first cultured monkey ES cells on PA6 stromal feeder cells, then detached the cells from the feeders for

**Nonstandard abbreviations used:** ChAT, choline acetyltransferase; DA, dopaminergic; DAT, dopamine transporter; GABA, γ-amino butyric acid; GalC, galactocerebroside C; GFAP, glial fibrillary acidic protein; GMEM, Glasgow minimum essential medium; i.m., intramuscular(ly); LIF, leukemia inhibitory factor; ME, mercaptoethanol; MPTP, 1-methyl-4-phenyl-1,2,3,6-tetrahydropyridine; NCAM, N cell adhesion molecule; OL, poly-l-ornithine and laminin; PD, Parkinson disease; PET, positron emission tomography; SDIA, stromal cell–derived inducing activity; TH, tyrosine hydroxylase.

**Conflict of interest:** The authors have declared that no conflict of interest exists.

**Citation for this article:** *J. Clin. Invest.* **115**:102–109 (2005). doi:10.1172/JCI200521137.

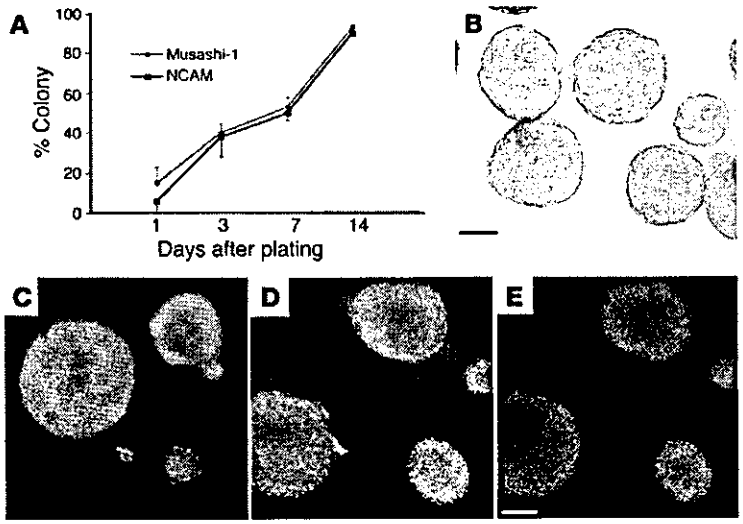


**Figure 1**
Neural progenitors induced from primate ES cells. (**A**) Time course of neural progenitor marker expression in monkey ES cells cultured on PA6 cells. (**B**) Detached ES cell colonies formed spheres similar to those of neural progenitor cells. (**C–E**) Spheres were immunoreactive for NCAM (**C**, green), Musashi-1 (**D**, red), and Nestin (**E**, green). Scale bar: 100 μm.

expansion as neurospheres. ES cells began to differentiate on PA6 cells, with cells immunoreactive for neural progenitor markers, such as N cell adhesion molecule (NCAM) and Musashi-1 (11, 14), emerging within three days. ES cells proliferated and differentiated on the feeder layer by forming colonies, and cells positive for neural markers increased in number until 2 weeks into the culture period. The percentages of the colonies including at least 1 NCAM- or Musashi-1-positive cell reached approximately 100% at 2 weeks of culture (NCAM = 90.4% ± 7.5%, Musashi-1 = 97.5% ± 4.6%, $n$ = 100 from 3 independent cultures; Figure 1A). At this time point, 78.3% ± 7.5% of the total cells were immunoreactive for NCAM, 75.0% ± 15.4% for Musashi-1, and 72.3% ± 9.1% for another neural progenitor marker, Nestin (14). These results indicate that the majority of the ES cells were committed to the neural lineage by day 14 of culture on feeder layers.

*In vitro characterization of neural progenitors derived from monkey ES cells.* To further enrich neural progenitors, we detached the ES cells from the feeder layer on day 14, then continued to culture the cells on noncoated dishes in serum-free medium containing FGF2, EGF, and leukemia inhibitory factor (LIF). During the next few days, the cells formed spheres morphologically resembling those formed by neural progenitor cells (Figure 1B). These spheres were positively stained with antibodies specific for neural progenitor cell markers NCAM, Musashi-1, and Nestin (Figure 1, C–E). To determine the potential of these cells to differentiate, we expanded the cells as spheres for 7 days, then induced differentiation by culturing the cells on poly-l-ornithine and laminin-coated (OL-coated) slides for 7 days. We removed the mitogens FGF2, EGF, and LIF from the medium, instead adding neurotrophic factors such as brain-derived neurotrophic factor and neurotrophin-3. Immunofluorescence analysis revealed that the cells differentiated into mature neural cells expressing the neuronal markers TuJ1 (52.8% ± 16.0% of DAPI) and Map2ab (38.3% ± 7.5% of DAPI), the astroglial marker glial fibrillary acidic protein (GFAP) (28.6% ± 17.6% of DAPI), and the oligodendroglial marker galactocerebroside C (GalC) (0.6% ± 0.4% of DAPI) (Figure 2, A–D and I). Further analyses demonstrated that these neurons derived from ES cells were immunoreactive for γ-amino butyric acid (GABA) (28.6% ± 10.7% of TuJ1), glutamate (14.3% ± 5.3% of TuJ1), choline acetyltransferase (ChAT) (0.7% ± 0.3% of TuJ1), and serotonin (3.3% ± 1.7% of TuJ1) (Figure 2, E–H and J). These results suggest that ES cell–derived spheres contain neural progenitor cells.

*Effect of growth factors on differentiation of DA neurons.* Effective treatment of PD requires substantial quantities of DA neurons. The percentage of tyrosine hydroxylase–positive (TH-positive) cells derived from neurospheres was only 5.4% ± 1.8% of the TuJ1-positive cells (Figure 2J). To increase the percentage of these cells, we examined the effects of various combinations of growth factors on neurosphere culture. The percentage of

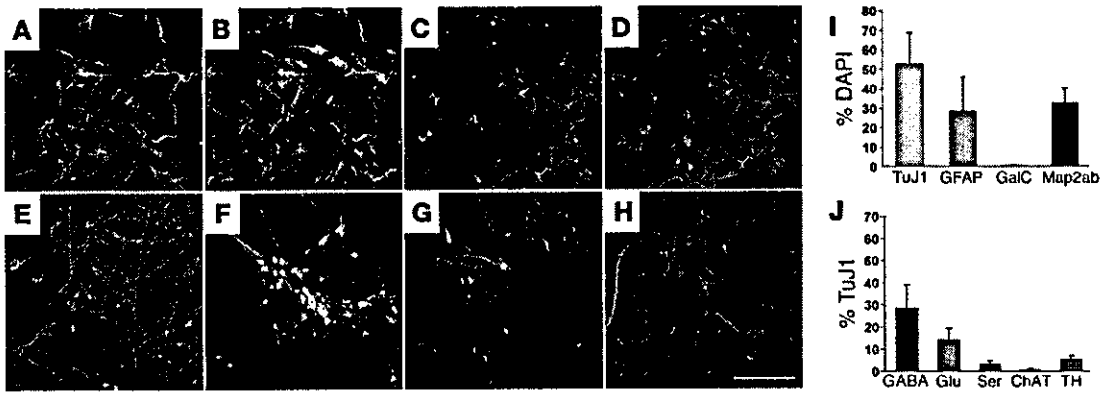


**Figure 2**
Expression of differentiated neural and neuronal subtype markers. Differentiated spheres were stained with antibodies against TuJ1 (**A** and **B**, green; **E–H**, blue), GFAP (**B**, red), Map2ab (**C** and **D**, green), GalC (**D**, red), GABA (**E**, red), glutamate (Glu; **F**, green), serotonin (Ser; **G**, red), and ChAT (**H**, green). Scale bar: 100 μm. The proportions of cells expressing differentiated neural (**I**) and neurotransmitter-related (**J**) markers are expressed as the mean ± SD of 3 independent cultures.

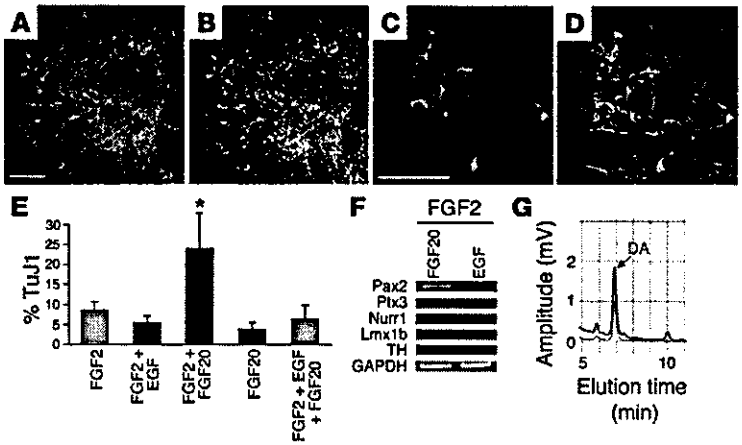


**Figure 3**
DA neurons differentiated from ES cell–derived neurospheres. (**A–D**) Differentiated spheres treated with FGF2 and FGF20 were stained with antibodies against TH (red) and TuJ1 (green). Scale bars: 50 μm. (**E**) The proportion of TH-positive cells to TuJ1-positive cells is expressed as the mean ± SD of 3 to 5 independent cultures. *$P < 0.05$. (**F**) RT-PCR for mesencephalic DA neuron markers *Pax2*, *Ptx3*, *Nurr1*, *Lmx1b*, and *TH* in cells treated with FGF2 and FGF20 (left) or FGF2 and EGF (right). (**G**) HPLC measuring concentration of dopamine released by SDIA- and FGF2- and FGF20-treated monkey ES cells in response to high $K^+$ depolarizing stimuli (blue line). Dopamine standard, red line.

TH-positive neurons out of total Tuj1-positive cells increased to 24% in the presence of FGF2 and FGF20 (Figure 3, A–E). Neither FGF2 nor FGF20 alone caused an increase in the number of TH-positive neurons. In the presence of FGF2, however, FGF20 increased the rate of TH differentiation in a dose-dependent manner (1 pg/ml = 3.8% ± 1.8% of TuJ1, 10 pg/ml = 8.8% ± 4.8% of TuJ1, 1 ng/ml = 24.3% ± 9.8% of TuJ1).

RT-PCR analyses showed that the cells derived from SDIA-induced neurospheres expressed mesencephalic DA neuron markers such as *Pax2*, *Ptx3*, *Nurr1*, *Lmx1b*, and *TH* (15, 16). The expression of these markers was more abundant in FGF2- and FGF20-treated cells than in FGF2- and EGF-treated cells (Figure 3F). Furthermore, FGF2- and FGF20-treated cells released 55.6 ± 19.9 pmol per $10^6$ cells of dopamine in response to high $K^+$ depolarizing stimuli as assayed by HPLC ($n = 5$; Figure 3G). These results indicate that monkey ES spheres treated both with SDIA and with FGF2 and FGF20 generate a significant number of functional DA neurons in vitro.

*Transplantation of DA neurons from ES-derived neural progenitors.* To determine if the isolated TH-positive neurons function as DA neurons in vivo, ES cell–derived neurospheres were grafted into the putamen of the monkeys with MPTP-induced PD. In this primate model of PD, we administered MPTP intravenously to *Macaca fascicularis* (cynomolgus monkeys), hereafter *M. fascicularis*, and evaluated their behavior by scoring for neurological symptoms, such as motility and tremor (Table 1). Only the animals that exhibited stable deterioration for periods longer than 12 weeks were used for transplantation. ES cell–derived neurospheres used for grafting were prepared by treating with SDIA for 14 days and, subsequently, with FGF2 and FGF20 for 7 days, as described above. Using MRI images obtained for each monkey, we determined the necessary coordinates to stereotactically transplant the cells (300,000–600,000 cells per side) into the bilateral putamen. After injection, we continuously analyzed the behavior of postoperative monkeys by assessing neurological scores. We observed a slight recovery in the behavioral symptoms even in the sham-operated animals. At 10 weeks after transplantation, however, the mean scores of ES cell–transplanted monkeys significantly improved over the levels observed in sham-operated ones (Figure 4A, $n = 6$ and 4, respectively). In our evaluation of symptoms after transplantation, posture recovery was the most prominent improvement seen in ES cell–transplanted monkeys, with significant improvements in motility also observed. There were, however, no significant changes in head-checking movement. Consciousness was not disturbed in any preoperative animals, and no deterioration was observed postoperatively. In addition, none of the treated animals developed dyskinesia. Positron emission tomography (PET) at 14 weeks after transplantation revealed increases in $^{18}$F-fluorodopa uptake at the putamen of the ES cell–transplanted animals (Figure 4, B and C).

After the PET study, animals were sacrificed and subjected to immunohistochemical analysis. Grafted cells, which were labeled by BrdU treatment during sphere culture, were detected in the putamen of ES cell–transplanted monkeys (7,996 ± 3,300 cells per side; Figure 5, A–C). DA neurons were detected by TH (Figure 5, B, C, E, and F; ref. 11) or dopamine transporter (DAT) (Figure 5, H and I; ref. 17) staining. An average of 2130 ± 645 TH-positive cells per side survived. Double labeling immunofluorescence microscopy revealed that 65.5% ± 4.3% and 50.3% ± 6.1% of the TH- and DAT-positive cells were immunoreactive for BrdU, respectively. Thus, the estimated number of TH/BrdU-double-positive cells was 1395 per side, 17.4% of the total of BrdU-positive cells. In contrast, in sham-operated monkeys, only a few TH-positive cells and scattered fibers were detectable in the putamen. No tumor formation or Ki-67–inducing reactivity was observed. As for other

**Table 1**
Neurological scores of MPTP-treated monkeys

| Behavior | Scores |
|---|---|
| Alertness | Normal, 0; reduced, 1; absent, 2 |
| Head-checking movement | Present, 0; reduced, 1; absent, 2 |
| Eyes | Normal, 0; reduced blinking, 1; eyes closed, 2 |
| Posture | Normal, 0; mildly abnormal, 1; abnormal, 2; grossly abnormal, 3 |
| Balance | Normal, 0; impaired, 1; frequent falling, 2; no movement, 3 |
| Motility, at rest | Normal, 0; mild bradykinesia, 1; bradykinesia, 2; akinesia, 3 |
| Motility, reaction to external stimuli | Normal, 0; mildly reduced, 1; reduced, 2; absent, 3 |
| Walking | Normal, 0; mildly reduced, 1; reduced, 2; no walking, 3 |
| Tremor | Absent, 0; mild/not always, 1; moderate, 2; severe, 3 |

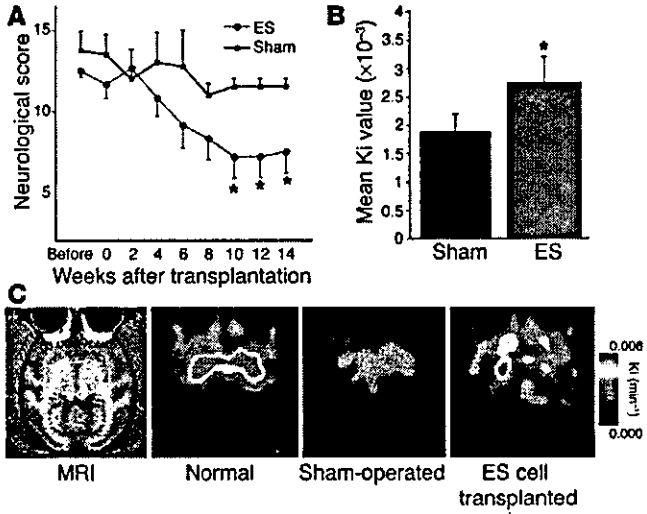


**Figure 4**
Function of ES cell–derived neurospheres in MPTP-treated monkeys. Behavioral scores (**A**) and PET study (**B** and **C**) of ES cell–transplanted ($n = 6$) and sham-operated animals ($n = 4$). (**B**) Mean Ki values from entire putamen. (**C**) Increased $^{18}$F-fluorodopa uptake in the putamen of ES cell–transplanted animals. All values are mean ± SD. $^*P < 0.05$.

neuronal phenotypes, GABA-positive cells were detected in the graft at a slightly higher frequency than TH-positive cells, while few serotonin-positive cells were present (data not shown).

## Discussion

Following initial work by Thomson et al. reporting a method for establishing primate ES cells (18), Suemori et al. (19) recently devised a similar scheme for generating *M. fascicularis* ES cells. Lee et al. recently reported a 5-step method to induce DA neurons from ES cells through the induction of neural progenitor cells from embryoid bodies (20). Transplantation of induced DA neurons derived from mouse ES cells improves the neurological symptoms of rats with a Parkinson-like syndrome induced by treatment with 6-hydroxydopamine (6-OHDA) (21). We have also reported a method of inducing DA neurons based on SDIA resulting from coculture of ES cells on a PA6 stromal feeder layer. By the use of this method, mouse ES cells are diverted to a neuronal fate with TH-positive DA neurons composing 30% of total TuJ1-positive neurons (10). Furthermore, this method produced similar results with *M. fascicularis* ES cells (11). In this study, we produced a highly enriched population of proliferating neural progenitors derived from SDIA-treated monkey ES cells. Furthermore, treatment of these cells with a combination of FGF2 and FGF20 induced the generation of a large population of DA neurons from ES cell–derived neural progenitors. Using MPTP-treated monkeys as a primate model for PD, we analyzed the effect of administration of DA neurons generated from monkey ES cells in vivo. Behavioral studies and functional imaging revealed that the transplanted cells functioned as DA neurons, attenuating the MPTP-induced symptoms.

In our preparation of graftable cells, we made two major modifications to our previously published protocol (10, 22). First, we induced the formation of neurospheres, expecting an enrichment of neuronal progenitor cells. We detached the ES cells from the feeder layer on day 14 and cultured them on noncoated dishes. Under these conditions, the cells formed floating spheres composed of neural precursor cells. Since the serum-free culture medium was suitable for neural cell growth, any contaminating nonneural and PA6 cells were likely eliminated as a result of a low proliferation rate and/or adherence to the bottom of the dish. Our previous report (22) demonstrated that, when grafted into the brain, fully maturated TH-positive neurons survived less efficiently than DA neuron progenitors induced by SDIA, probably due to their susceptibility to mechanical stress. This result is consistent with the fact that transplantation of mesencephalon tissues from early gestation stage embryos undergoing neurogenesis of DA neurons resulted in good survival of TH-positive cells (1300–18,000) and increased dopamine concentrations in the caudate nucleus of MPTP-treated monkeys, whereas these effects are not observed when mesencephalon tissues from later stages are transplanted (23). Thus, ES cell–derived neuronal progenitors competent to generate DA neurons appear to be more suitable for transplantation than DA neurons matured in vitro.

Another important modification to our previous protocol is the use of FGF2 and FGF20 treatment to enhance the generation of DA neurons. The percentage of TH-positive neurons generated from

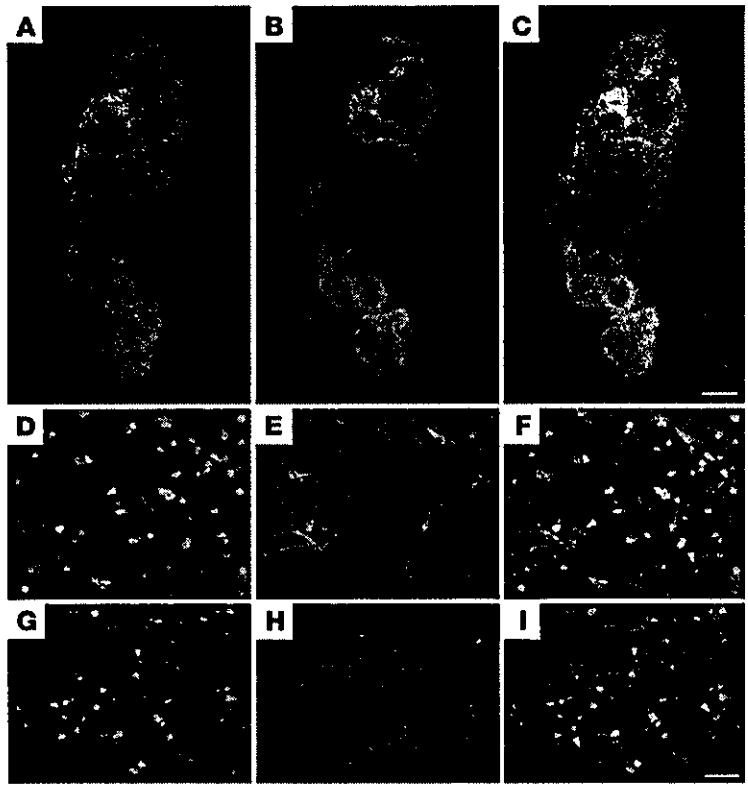


**Figure 5**
Survival of ES cell–derived DA neurons in the striatum. (**A–C**) Grafted cells (BrdU-labeled, green) survived and differentiated into DA neurons (TH-positive, red) along the needle tract (merged image **C**). Scale bar: 500 μm. (**D–I**) Colocalization (arrows in **F** and **I**) of BrdU (**D**, **F**, **G**, and **I**, green) and TH (**E** and **F**, red) or DAT (**H** and **I**, red) shows that graft-derived cells have dopaminergic character. Scale bar: 50 μm.